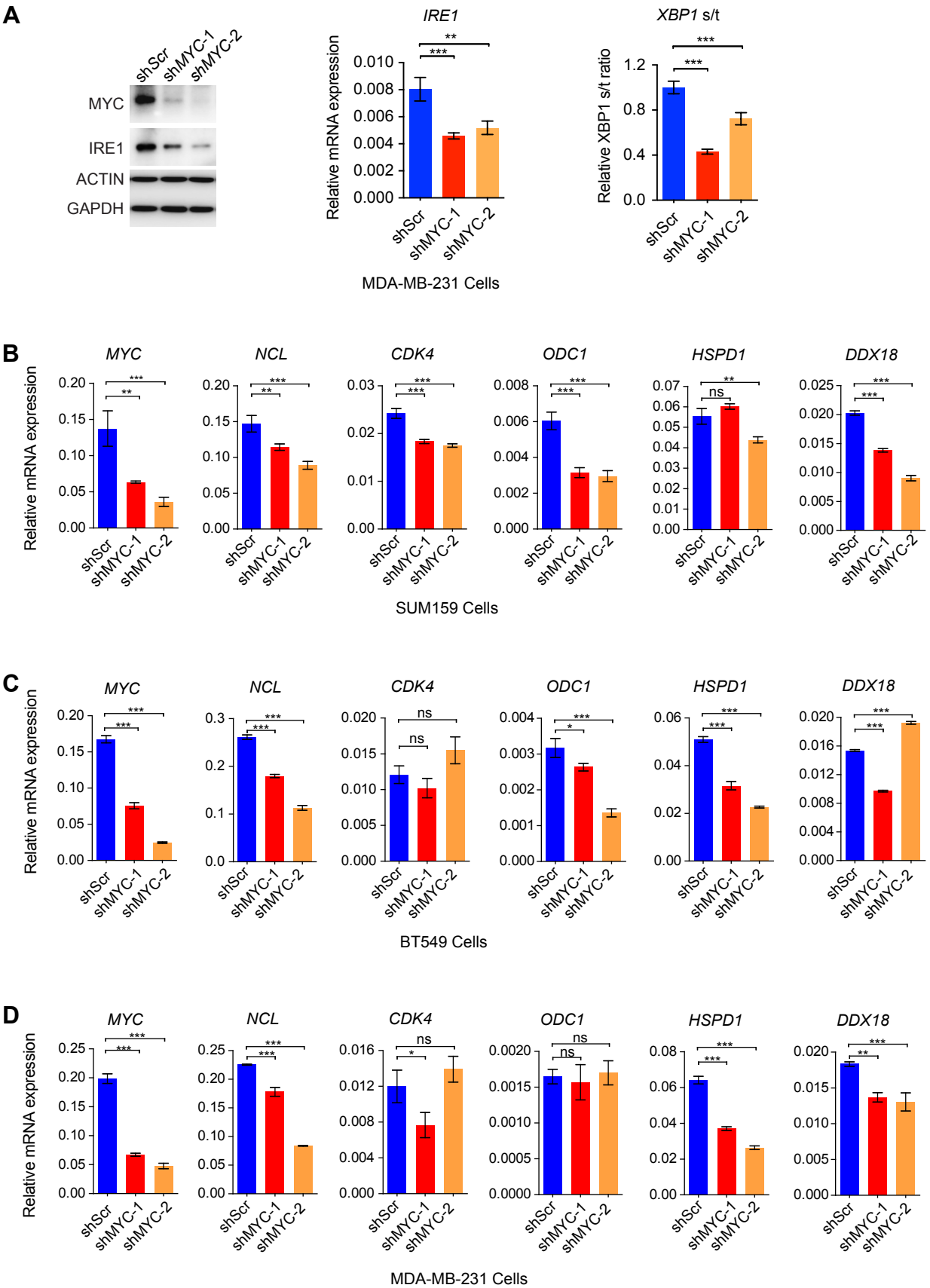

Supplemental Figure 1. MYC is necessary for activation of the IRE1/XBP1 pathway.
(**A**) MDA-MB-231 cells were infected with lentiviruses encoding control shRNA (sh*Scr*) or two distinct MYC shRNAs (sh*MYC*-1 and sh*MYC*-2). Left, Immunoblot of MYC and IRE1 in whole cell lysates. ACTIN and GAPDH were used as loading control. Middle, qRT-PCR analysis of *IRE1* expression. Data are presented relative to *ACTIN* and shown as mean ± s.d. of technical triplicates. Right, qRT-PCR analysis of *XBP1* splicing. *XBP1* s/t: the ratio of *XBP1s* to total *XBP1* (*XBP1t*). The *XBP1* s/t ratio was normalized to that of the scramble (sh*Scr*) control. Data are presented as mean ± s.d. of technical triplicates. (**B-D**) qRT-PCR analysis of *MYC* and MYC target genes in SUM159 (**B**), BT549 (**C**) and MDA-MB-231 (**D**) cells infected with lenti-viruses encoding control shRNA (sh*Scr*) or two distinct *MYC* shRNAs (sh*MYC*-1 and sh*MYC*-2). Data are presented relative to *ACTIN* and shown as mean ± s.d. of technical triplicates. All results shown are representative of three independent experiments. p value was calculated using one-way ANOVA with Turkey's multiple comparison test. ns, not significant; * $p<0.05$; ** $p<0.01$; *** $p<0.001$.

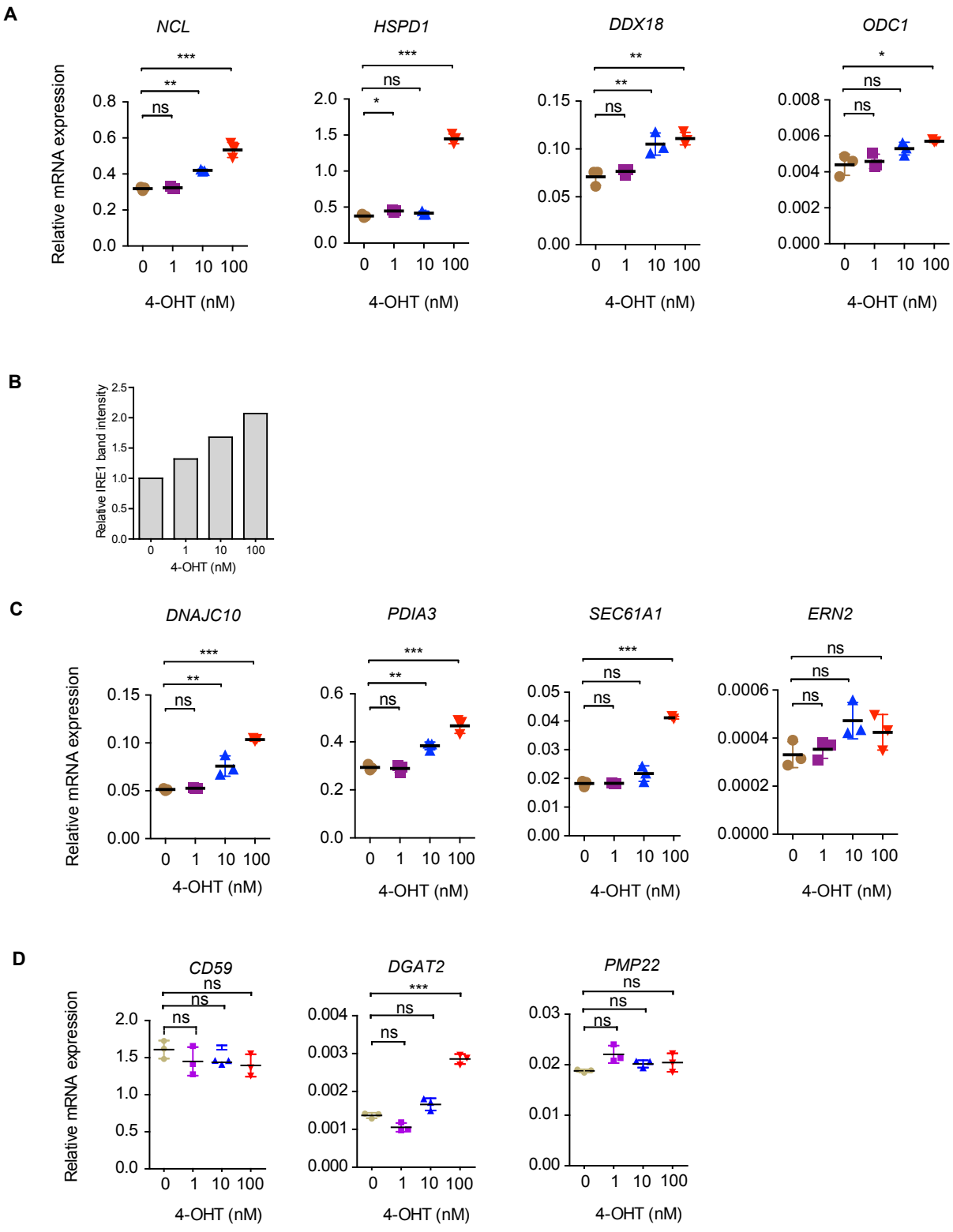

Supplemental Figure 2. MYC induces the expression of XBP1 target genes.
(**A**) qRT-PCR analysis of MYC target genes expression in MCF10A^{MYC-ER} cells treated with different doses of 4-OHT for 24 h. (**B**) Intensity analysis of IRE1 immunoblot band in Figure 2B using ImageJ software. The IRE1 band intensity was divided by the sum of ACTIN and GAPDH band intensities and normalized to that of the vehicle-treated group. (**C**, **D**) qRT-PCR analysis of UPR genes (**C**) and RIDD targets (**D**) expression in MCF10A^{MYC-ER} cells that were treated with different doses of 4-OHT for 24 h. In (**A**, **C**, **D**), data are presented relative to *ACTIN* and shown as mean ± s.d. of technical triplicates. All results shown are representative of three independent experiments. p value was calculated using one-way ANOVA with Turkey's multiple comparison test. ns, not significant; * p<0.05; ** p<0.01; *** p<0.001.

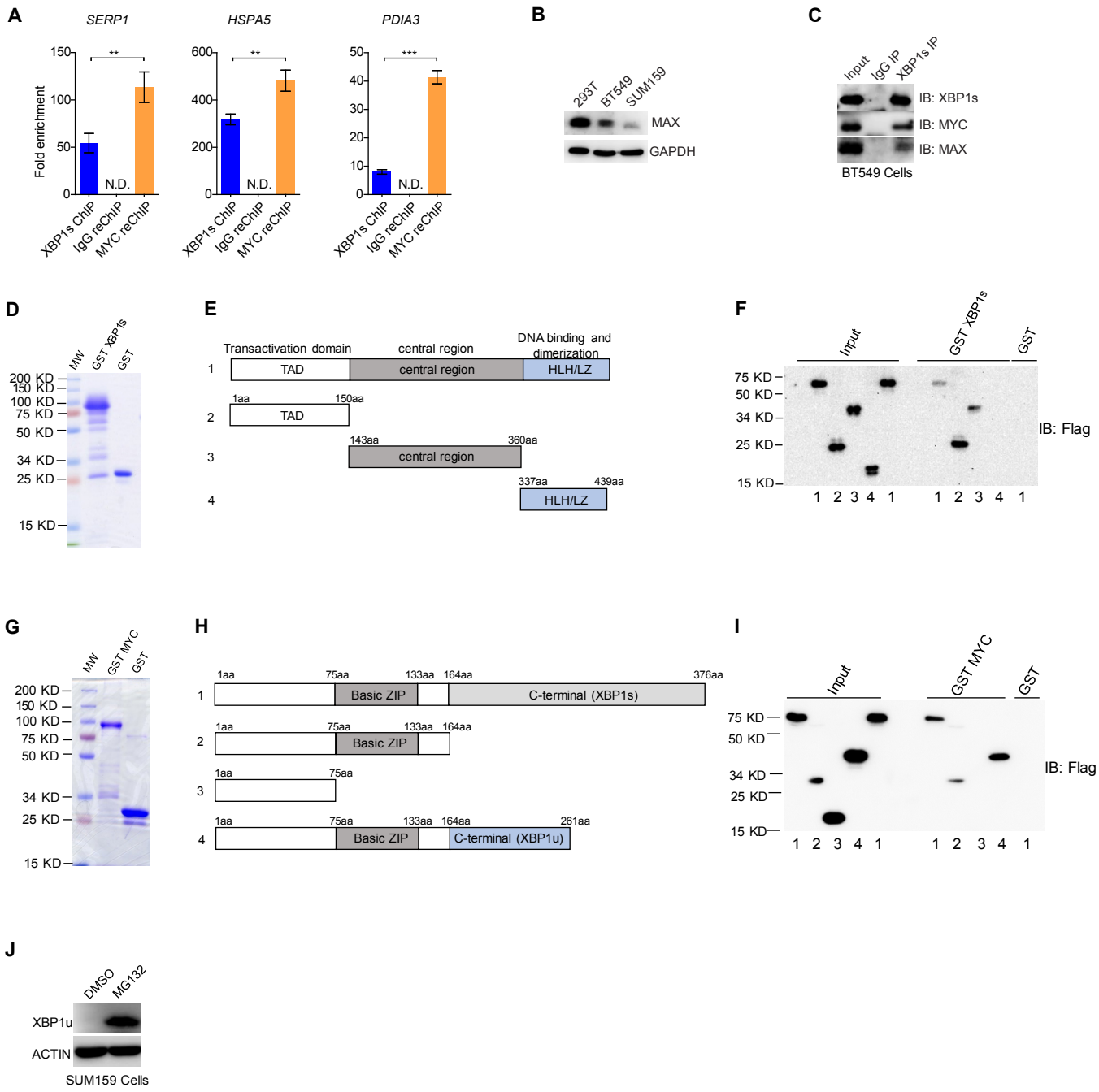

Supplemental Figure 3. MYC interacts with XBP1.

(**A**) ChIP-re-ChIP assay of tunicamycin-treated SUM159 cells was performed using the anti-XBP1s antibody first (XBP1s ChIP), the eluents were subjected to a second ChIP assay using IgG (IgG reChIP) or anti-MYC antibody (MYC reChIP) to detect enriched gene promoter fragments. N.D., not detected by qPCR assay. Data are shown as mean ± s.d. of technical triplicates. p value was calculated using two-tailed unpaired Student's t-test. ** $p<0.01$; *** $p<0.001$. (**B**) Immunoblot of MAX in 293T, BT549 and SUM159 cell lines. GAPDH was used as loading control. (**C**) Nuclear extracts from tunicamycin-treated BT549 cells were subjected to co-IP with anti-XBP1s antibody. The immunoblot was probed with anti-XBP1s, anti-MYC, and anti-MAX antibodies. Normal IgG was used as negative control. (**D**) Coomassie blue staining of GST protein and GST-tagged XBP1s protein. (**E**) Schematic diagram of full-length (1) and truncated forms (2, 3, 4) of Flag-tagged MYC proteins. (**F**) GST pull-down assay was performed using GST-tagged XBP1s or GST protein and 293T cell lysates overexpressing Flag-tagged full-length (1) and truncated forms (2, 3, 4) of MYC proteins. Immunoblotting was performed with anti-Flag antibody. (**G**) Coomassie blue staining of GST protein and GST-tagged MYC protein. (**H**) Schematic diagram of full-length and truncated forms of Flag-tagged XBP1s and XBP1u proteins. (**I**) GST pull-down assay was performed using GST-tagged MYC protein or GST protein and 293T cell lysates overexpressing Flag-tagged full-length XBP1s (1), full-length XBP1u (4) and truncated forms XBP1 (2, 3) proteins. Immunoblotting was performed with anti-Flag antibody. (**J**) Immunoblot of XBP1u in SUM159 cells treated with DMSO or 10 μM MG132 for 6 h. ACTIN was used as loading control.

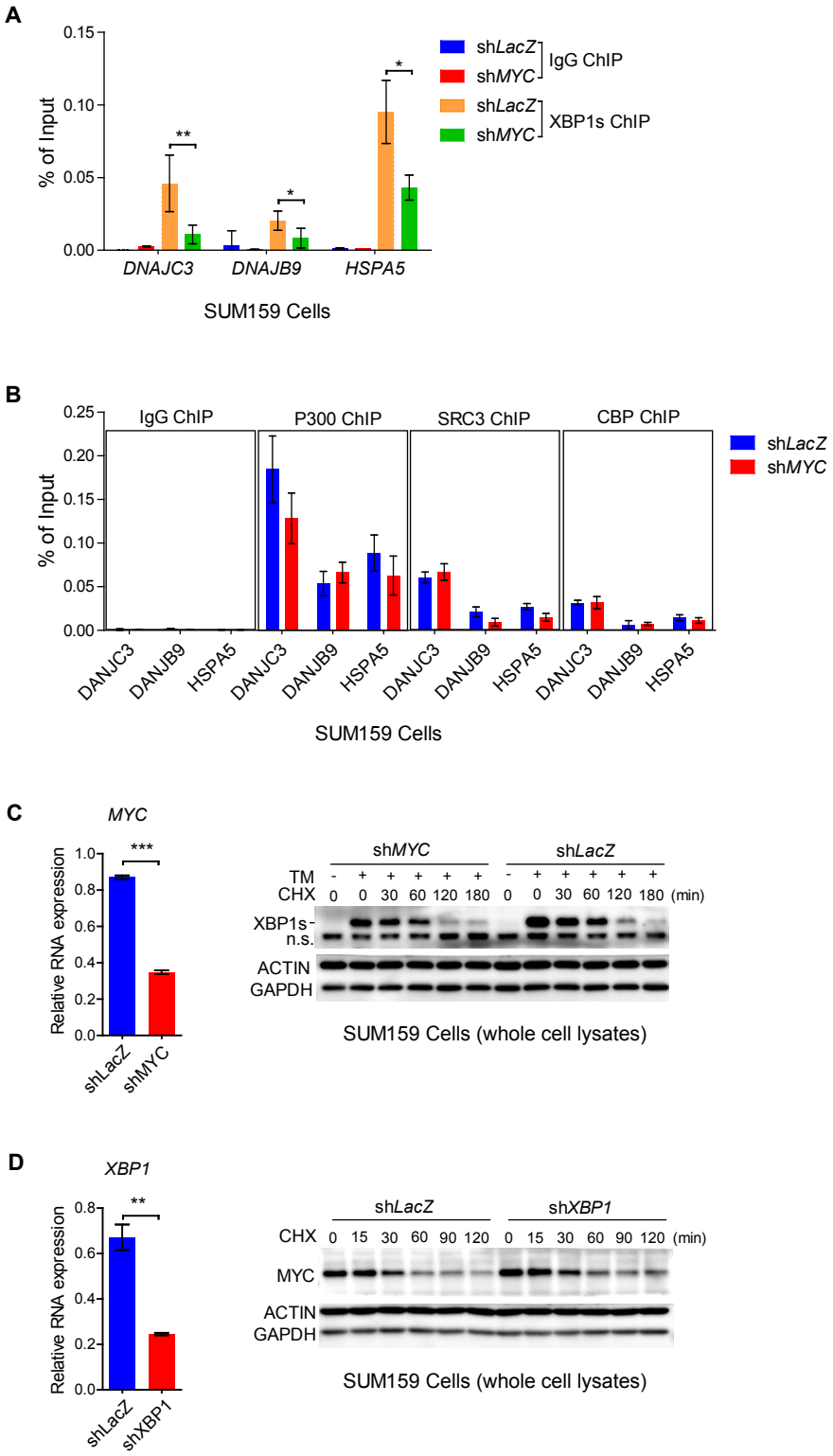

Supplemental Figure 4. MYC promotes XBP1s binding to its target genes.
(**A**) SUM159 cells were infected with lentiviruses encoding control shRNA (sh*LacZ*) or *MYC* shRNA (sh*MYC*). ChIP assays were performed using anti-XBP1s antibody to detect enriched gene promoter fragments. (**B**) SUM159 cells were infected with lentiviruses encoding control shRNA (sh*LacZ*) or *MYC* shRNA (sh**MYC**). ChIP assays were performed using anti-P300, anti-SRC3 or anti-CBP antibodies to detect enriched gene promoter fragments. In (**A**, **B**), IgG was used as mock control. Data are presented relative to input and shown as mean ± s.d. of technical triplicates. (**C**) SUM159 cells were infected with lentiviruses encoding control shRNA (sh*LacZ*) or *MYC* shRNA (sh*MYC*) and treated with 100 μg/ml Cycloheximide (CHX) for various periods in the presence of DMSO or 5 μg/ml tunicamycin (TM). Left, qRT-PCR analysis of MYC expression. Right, immunoblot of XBP1s. n.s. indicates non-specific band. (**D**) SUM159 cells were infected with lentiviruses encoding control shRNA (sh*LacZ*) or *XBP1* shRNA (sh*XBP1*) and treated with 100 μg/ml CHX for various periods. Left, qRT-PCR analysis of *XBP1* expression. Right, immunoblot of MYC. In (**C**, **D**), ACTIN and GAPDH were used as loading control in immunoblot assays. qPCR Data are presented relative to *ACTIN* and shown as mean ± s.d. of technical triplicates. In (**A**, **C**, **D**), p value was calculated using two-tailed unpaired Student's t-test. * $p<0.05$; ** $p<0.01$; *** $p<0.001$.

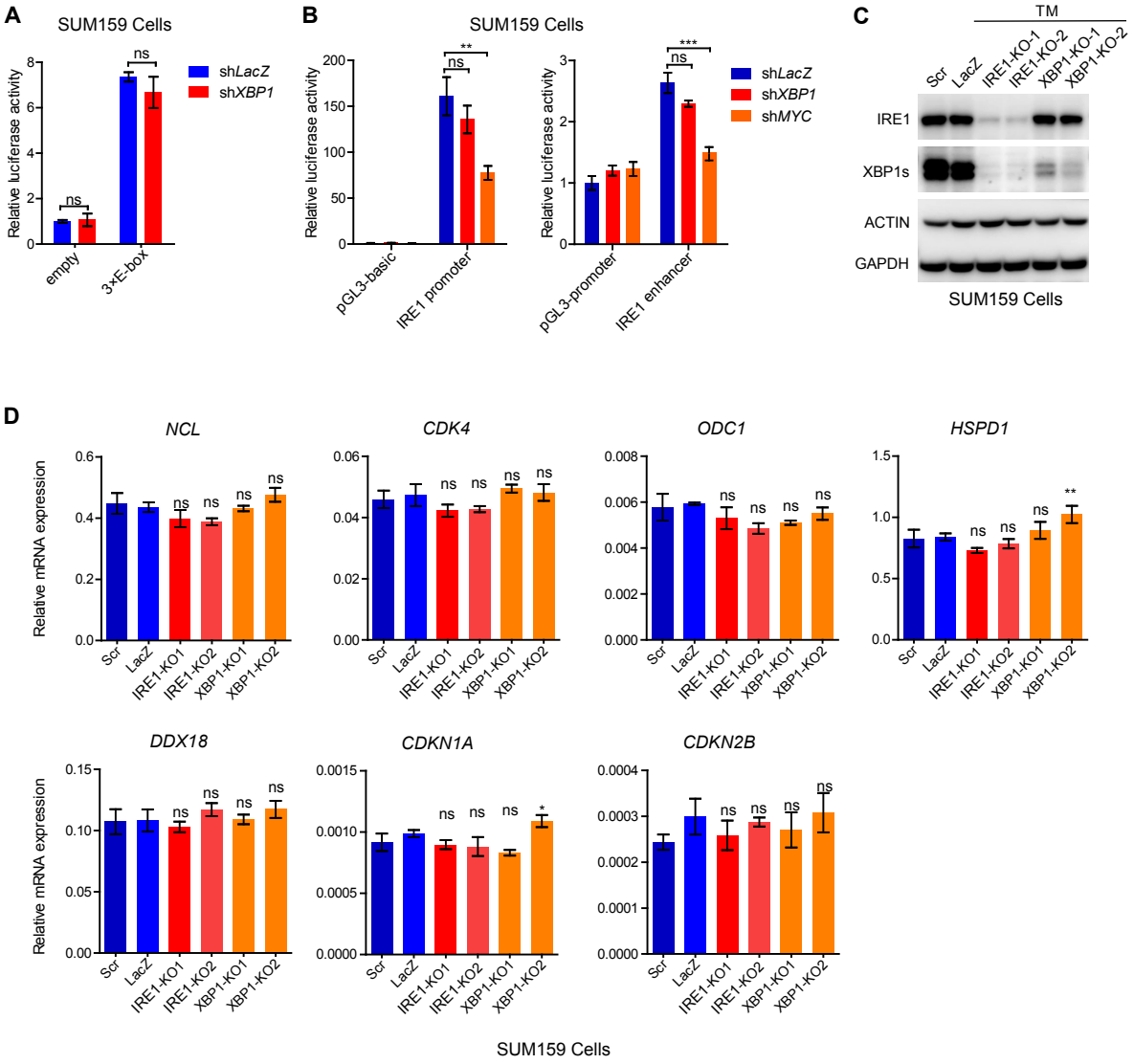

Supplemental Figure 5. The IRE1/XBP1 pathway does not affect MYC and MYC-MIZ1 transcriptional program in SUM159 cells.

(**A**) 3×E-Box luciferase reporter was transfected into SUM159 cells infected with lentiviruses encoding control shRNA (sh*LacZ*) or *XBP1* shRNA (sh*XBP1*), and luciferase activity was measured 48 h post transfection. (**B**) *IRE1* promoter or enhancer luciferase reporter was transfected into SUM159 cells infected with lentiviruses encoding control shRNA (sh*LacZ*), *XBP1* shRNA (sh*XBP1*), or *MYC* shRNA (sh*MYC*), and luciferase activity was measured 48 h post transfection. pGL3-basic or pGL3-promoter is empty vector control for *IRE1* promoter or enhancer reporter, respectively. In (**A**, **B**), data are presented relative to Renilla readings and shown as mean ± s.d. of biological triplicates. (**C**) SUM159-iCas9 cells were infected with lentiviruses encoding control gRNA (*Scr* or *LacZ)*, two distinct *IRE1* double gRNA constructs (*IRE1*-KO-1, *IRE1*-KO-2), or two distinct *XBP1* double gRNA constructs (*XBP1*-KO-1, *XBP1*-KO-2). Immunoblot of IRE1 and XBP1s were performed in multiclonal cells treated with 5 µg/ml tunicamycin (TM) for 4 h. ACTIN and GAPDH were used as loading controls. (**D**) qRT-PCR analysis of MYC and MYC-MIZ1 target genes in SUM159-iCas9-KO multiclonal cells. Data are presented relative to *ACTIN* and shown as mean ± s.d. of technical triplicates. All results shown are representative of two independent experiments. p value was calculated using two-tailed unpaired Student's t-test (**A**) or one-way ANOVA with Turkey's multiple comparison test (**B**, **D**). ns, not significant; * p<0.05; ** p<0.01; *** p<0.001.

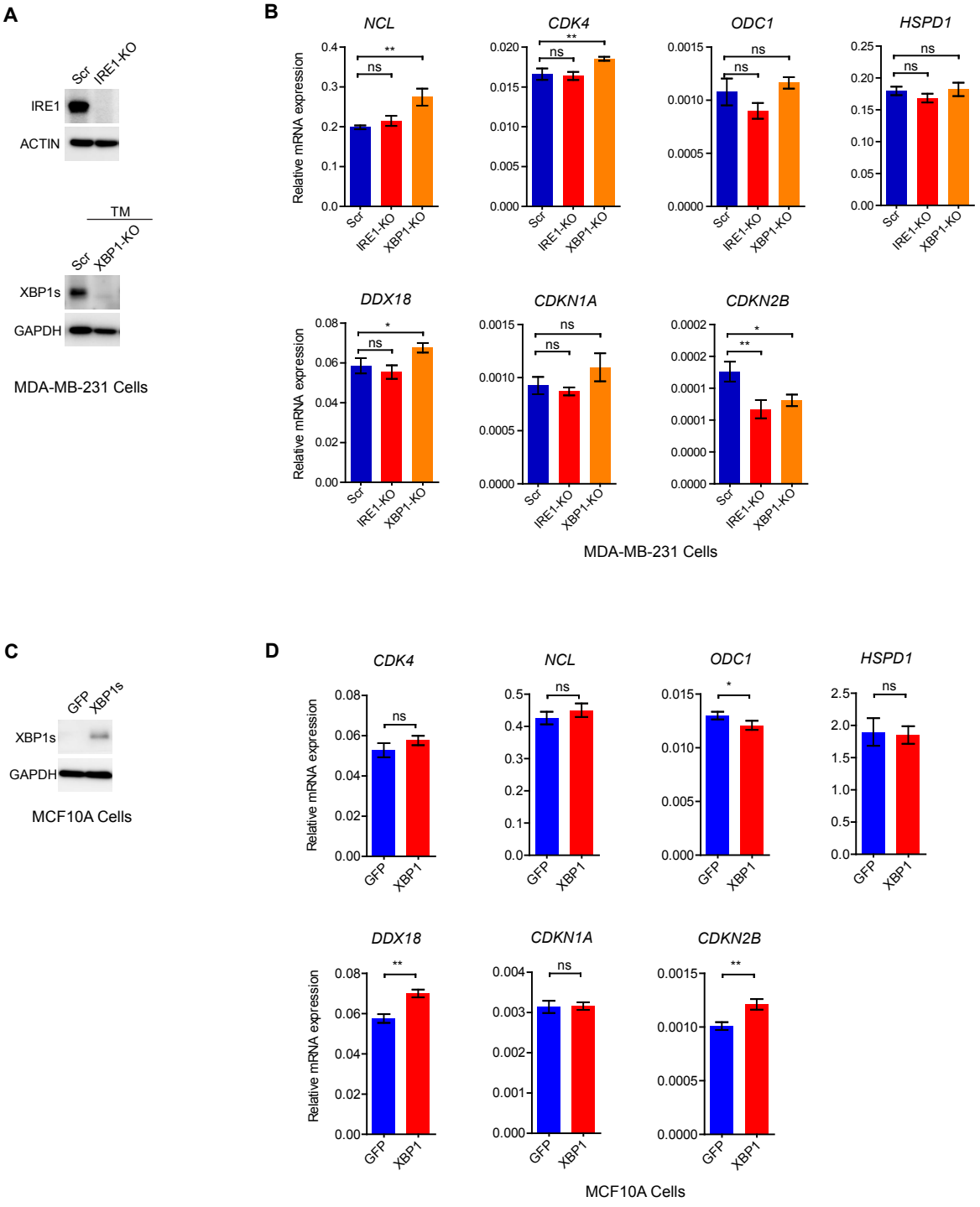

Supplemental Figure 6. The IRE1/XBP1 pathway does not affect MYC and MYC-MIZ1 transcriptional program in MDA-MB-231 and MCF10A cells.

(**A**) Immunoblot of IRE1 and XBP1s in whole cell lysates of pooled MDA-MB-231 KO cells. To detect XBP1s, cells were treated with 5 µg/ml tunicamycin (TM) for 4 h. ACTIN were used as loading controls. (**B**) qRT-PCR analysis of MYC and MYC-MIZ1 target genes in pooled MDA-MB-231 KO cells. (**C**) Immunoblot of XBP1s in MCF10A^{MYC-ER} cells infected with lentiviruses encoding GFP or XBP1s. GAPDH were used as loading controls. (**D**) qRT-PCR analysis of MYC and MYC-MIZ1 target genes in MCF10A^{MYC-ER} cells infected with lentiviruses encoding GFP or XBP1s. In (**B**, **D**), data are presented relative to *ACTIN* and shown as mean ± s.d. of technical triplicates. p value was calculated using one-way ANOVA with Turkey's multiple comparison test (**B**) or two-tailed unpaired Student's t-test (**D**). ns, not significant; * $p<0.05$; ** $p<0.01$; *** $p<0.001$.

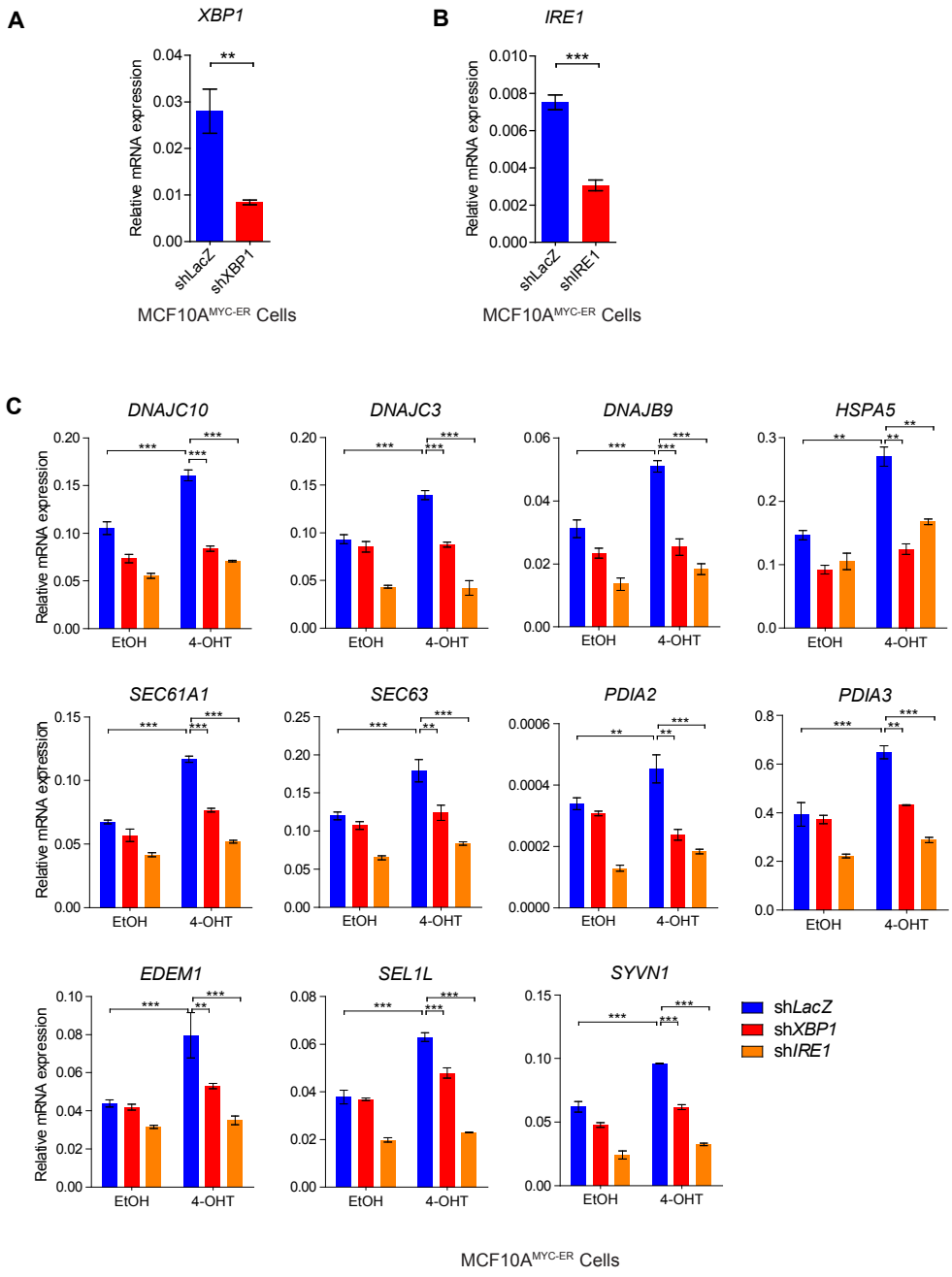

Supplemental Figure 7. MYC promotes IRE1/XBP1 dependent UPR gene expression.
(**A**, **B**) qRT-PCR analysis of *XBP1* (**A**) or *IRE1* (**B**) expression in MCF10A^{MYC-ER} cells infected with lentiviruses encoding control shRNA (sh*LacZ*), *XBP1* shRNA (sh*XBP1*) or *IRE1* shRNA (sh*IRE1*). (**C**) qRT-PCR analysis of UPR downstream gene expression in MCF10A^{MYC-ER} cells infected with lentiviruses encoding control shRNA (sh*LacZ*), *XBP1* shRNA (sh*XBP1*) or *IRE1* shRNA (sh*IRE1*) and treated with EtOH or 100 nM 4-OHT for 24 h. Data are presented relative to *ACTIN* and shown as mean ± s.d. of technical triplicates. p value was calculated using two-tailed unpaired Student's t-test (**A**, **B**) or one-way ANOVA with Turkey's multiple comparison test (**C**). ** p<0.01; *** p<0.001.

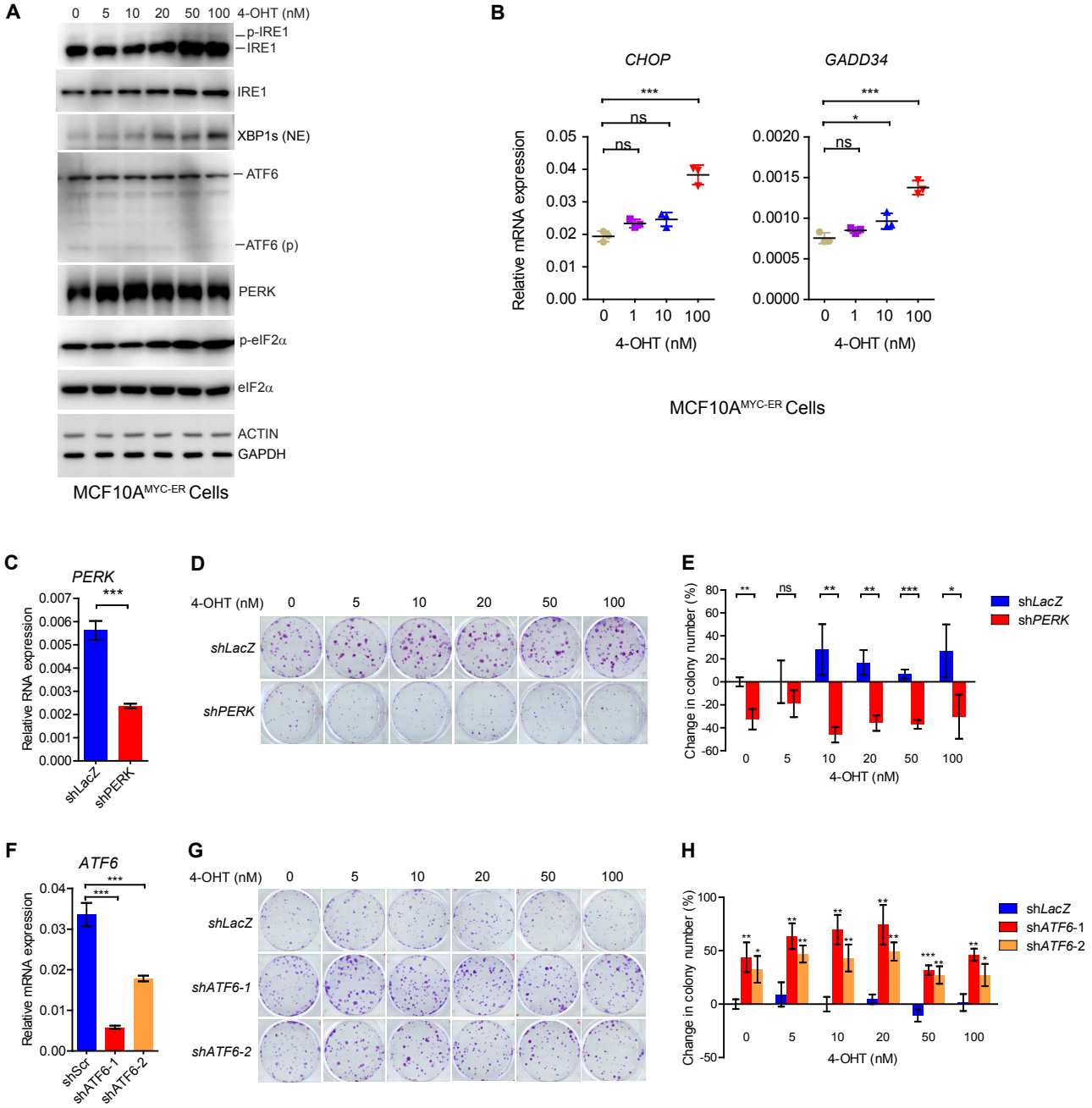

Supplemental Figure 8. Impact of PERK and ATF6 on the clonogenic growth of MYC-hyperactivated cells.
(**A**) Immunoblot of IRE1 phosphorylation (phos-tag SDS-PAGE), XBP1s, ATF6 cleavage (ATF6p), PERK phosphorylation, and eIF2α phosphorylation in MCF10A^{MYC-ER} cells treated with different doses of 4-OHT for 24 h. XBP1s was detected from nuclear extracts (NE). ACTIN and GAPDH were used as loading control for whole cell lysates. (**B**) qRT-PCR analysis of *CHOP* and *GADD34* expression in MCF10A^{MYC-ER} cells treated with different doses of 4-OHT for 24 h. (**C-H**) Clonogenic survival and growth of MCF10A^{MYC-ER} cells infected with lentiviruses encoding shRNAs against *LacZ* control, *PERK* (**C-E**), or *ATF6* (**F-H**). The cells were treated with different doses of 4-OHT (to induce MYC-ER translocation). Ethanol was used as vehicle control for 4-OHT. (**C**, **F**) qRT-PCR analysis of knockdown efficiency in MCF10A^{MYC-ER} cells. (**D**, **G**) Representative images of cell colonies. (**E**, **H**) Quantification of changes in colony number. Changes in colony number were compared with vehicle-treated MCF10A^{MYC-ER} cells expressing sh*LacZ*. Data are presented as mean ± s.d. of biological triplicates. In (**B**, **C**, **F**), qRT-PCR data are presented relative to *ACTIN* and shown as mean ± s.d. of technical triplicates. All data shown are representative of two independent experiments. p value was calculated using one-way ANOVA with Turkey's multiple comparison test (**B**, **F**, **H**) or two-tailed unpaired Student's t-test (**C**, **E**). ns, not significant; * p<0.05; ** p<0.01; *** p<0.001.

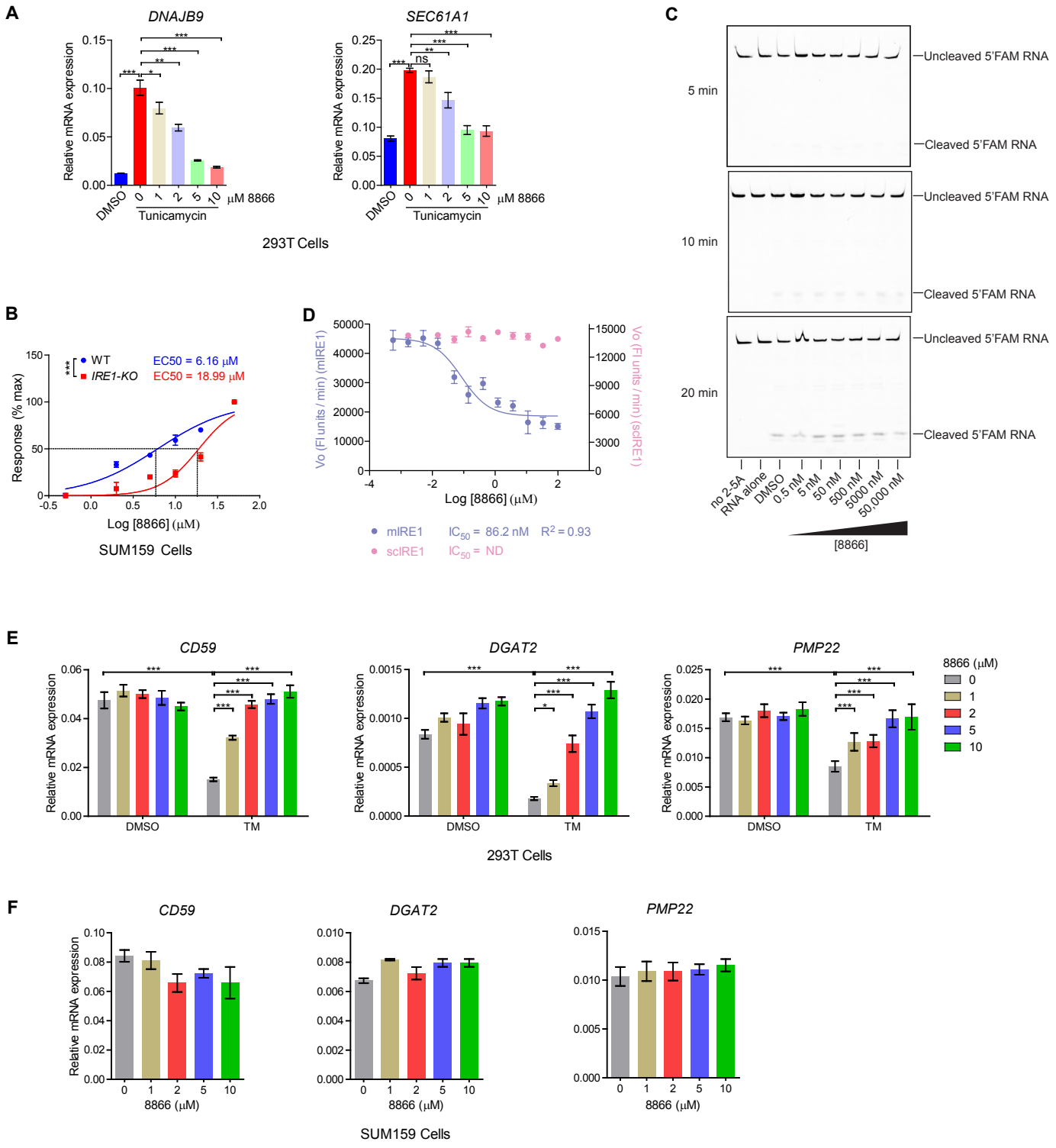

Supplemental Figure 9. Characterization of IRE1 RNase inhibitor 8866.
(**A**) qRT-PCR analysis of XBP1 target genes in 293T cells that were treated with different doses of 8866 in the presence of DMSO or 5 μg/ml tunicamycin for 6 h. (**B**) Concentration-response curves of 8866 in WT or multiclonal *IRE1*-KO SUM159 cells. The EC50 values were estimated using nonlinear regression analysis. (**C**) Effect of 8866 on the RNase activity of RNase L using an RNA substrate labeled with 6-FAM and BHQ1 on its 5' and 3' termini, respectively. Cleavage reactions were monitored at 5, 10 and 20 min and the samples were run on a UREA-TBE RNA gel. No RNase L activator (no 2-5A) or no enzyme (RNA alone) groups served as negative controls. (**D**) Inhibition profiles of murine IRE1 (mIRE1) and yeast IRE1 (scIRE1) RNase activity by 8866 using FRET assay. IC50 values were estimated using nonlinear regression analysis. (**E**) qRT-PCR analysis of RIDD targets expression in 293T cells treated with different doses of 8866 in the presence of DMSO or 5 μg/ml tunicamycin (TM) for 6 h. (**F**) qRT-PCR analysis of RIDD targets expression in SUM159 cells treated with different doses of 8866 for 24 h. In (**A**, **E**, **F**), qRT-PCR data are presented relative to *ACTIN* and shown as mean ± s.d. of technical triplicates. p value was calculated using one-way ANOVA with Turkey's multiple comparison test (**A**, **E**), or extra sum-of-squares F test (**B**). ns, not significant; * p<0.05; ** p<0.01; *** p<0.001.

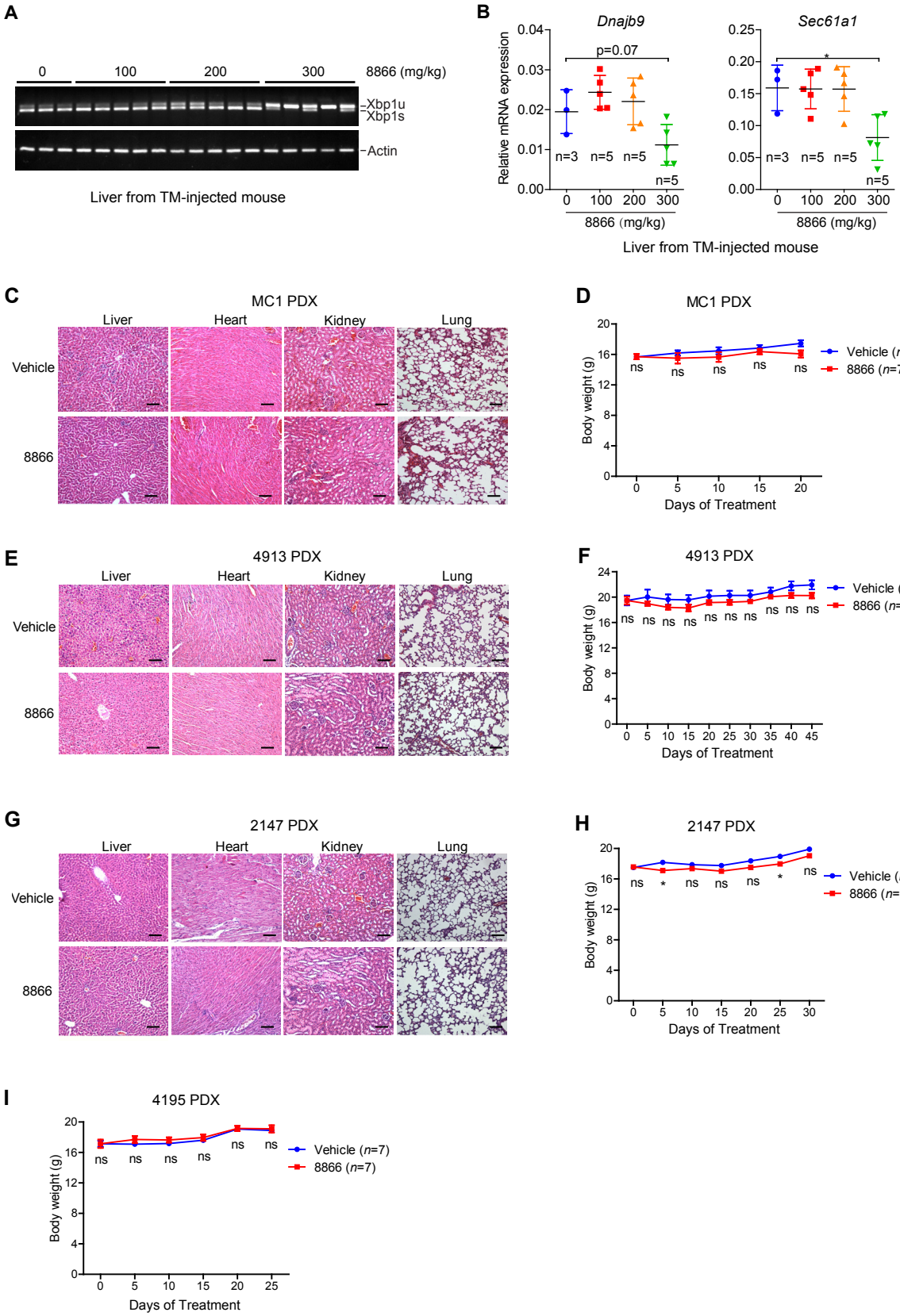

Supplemental Figure 10. The 8866 treatments do not cause obvious toxicity in PDX tumor-bearing mice.
(**A**, **B**) 8866 inhibits *Xbp1* splicing in vivo. RT-PCR analysis of *Xbp1* splicing (**A**) and Xbp1 targets expression (**B**) in livers tissue of C57BL/6 mice that were treated with either vehicle or 8866 through oral gavage for 24 h. All mice received tunicamycin (TM) through i.p. injection 6 h prior to sacrifice. qPCR data are presented relative to *Actin* and shown as mean ± s.d. of biological replicates. p value was calculated using two-tailed unpaired Student's t-test. * p<0.05. (**C-I**) Toxicity analysis of MC1 (**C**, **D**), 4913 (**E**, **F**), 2147 (**G**, **H**) and 4195 (**I**) PDX-bearing SCID/Beige mice treated with vehicle or 8866 via daily oral gavage at 300 mg/kg dose. (**C**, **E**, **G**) H&E staining of liver, heart, kidney and lung of treated mice harvested at the end of the experiments. Scale bar, 50 µm. (**D**, **F**, **H**, **I**) Body weight of mice treated with 8866. In **D**, **F**, **H** and **I**, data are presented as mean ± s.e.m of biological replicates. p value was calculated using two-way ANOVA with Bonferroni posttest. ns, not significant; * p<0.05.

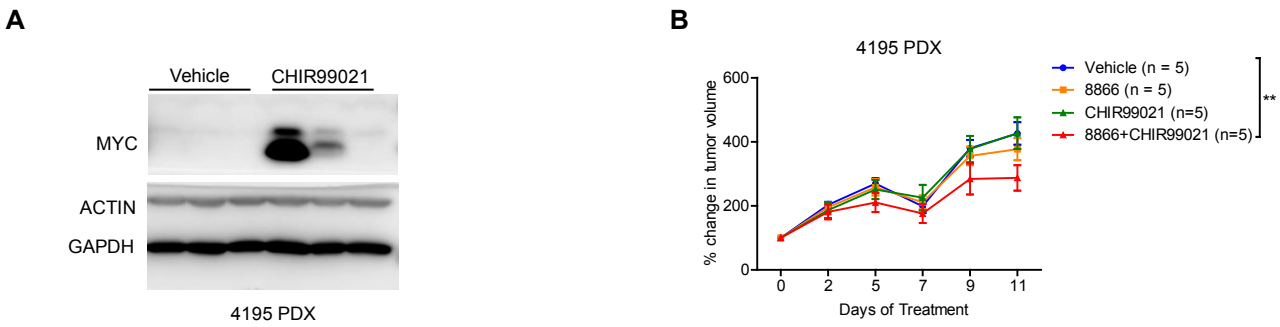

Supplemental Figure 11. Increasing MYC level in 4195 PDX model sensitizes the tumors to 8866 treatment. (**A**) Immunoblot of MYC in tissue lysates of 4195 PDX tumors treated with vehicle or CHIR99021 (30 mg/kg, i.p. injection every two days). ACTIN and GAPDH were used as loading control. n=3 in each group. (**B**) Quantification of tumor volume change of established 4195 PDX tumors in SCID/Beige mice treated with vehicle, 8866, CHIR99021 or 8866 + CHIR99021 (*n*=5). Data are presented as mean ± s.e.m of biological replicates. p value was calculated using two-way ANOVA with Bonferroni posttest. ** $p<0.01$.

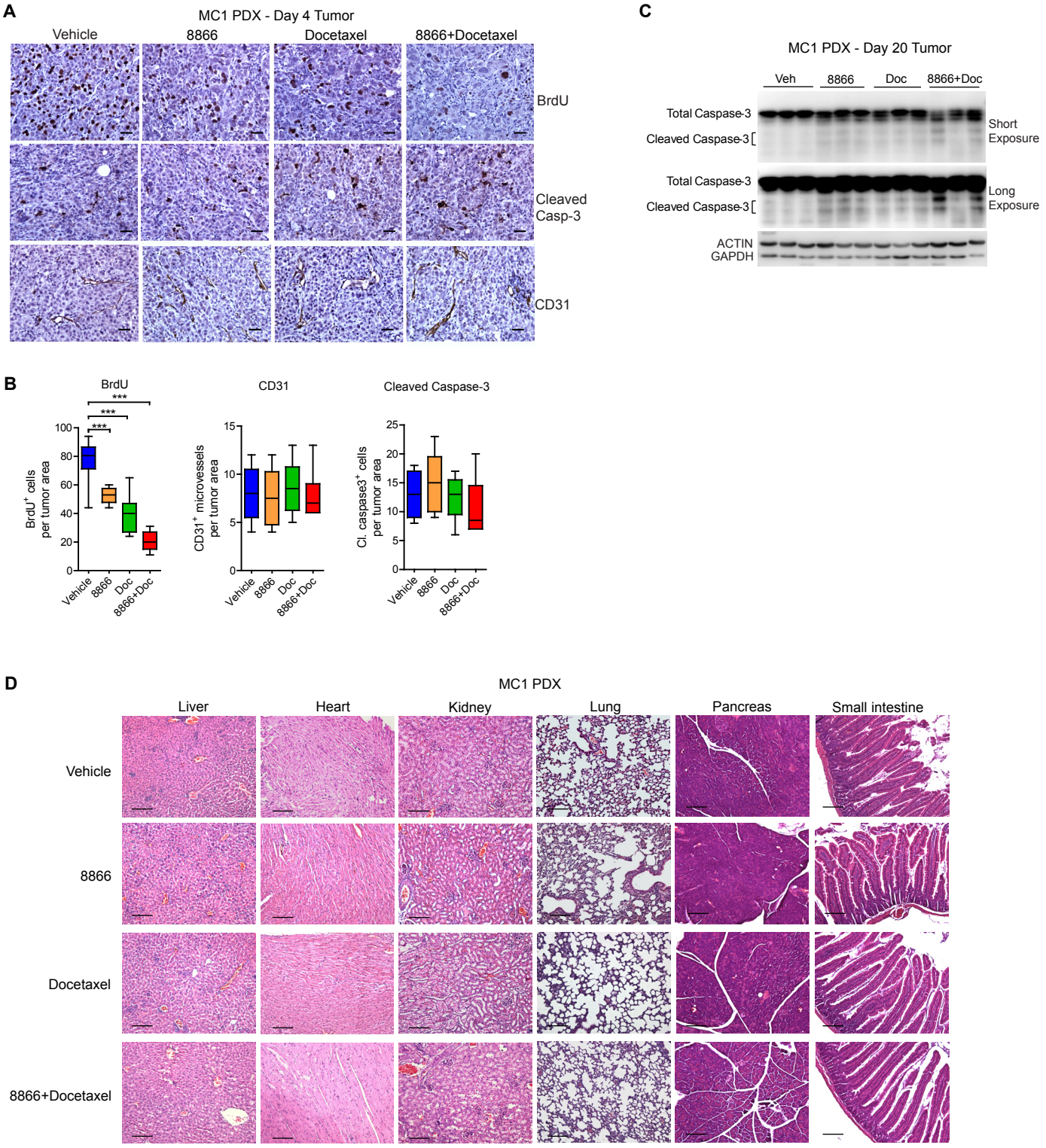

Supplemental Figure 12. The effect of 8866 +/- docetaxel treatments on MC1 PDX tumor.
(**A**) BrdU, cleaved Caspase-3 and CD31 immunostaining images of MC1 PDX tumors treated with vehicle, 300 mg/kg 8866 (daily oral gavage), docetaxel (10 mg/kg, weekly i.p. injection), or the combination of 8866 and docetaxel for 4 days. Scale bar, 50 µm. (**B**) Quantification of BrdU positive cells, CD31 positive microvessels or cleaved Caspase-3 positive cells on tumor sections stained in (**A**). More than 10 tumor areas from each group were counted. Doc: docetaxel. p value was calculated using one-way ANOVA with Turkey's multiple comparison test. *** $p<0.001$. (**C**) Immunoblot of Caspase-3 in tissue lysates of MC1 PDX tumors treated with vehicle, 300 mg/kg 8866 (daily oral gavage), docetaxel (10 mg/kg, weekly i.p. injection), or the combination of 8866 and docetaxel for 20 days. Mice undergoing monotherapy also received vehicle. *n*=3 in each group. (**D**) H&E staining of liver, heart, kidney, lung, pancreas and small intestine of MC1 PDX-bearing SCID/Beige mice treated as in (**C**). Scale bar, 50 µm.

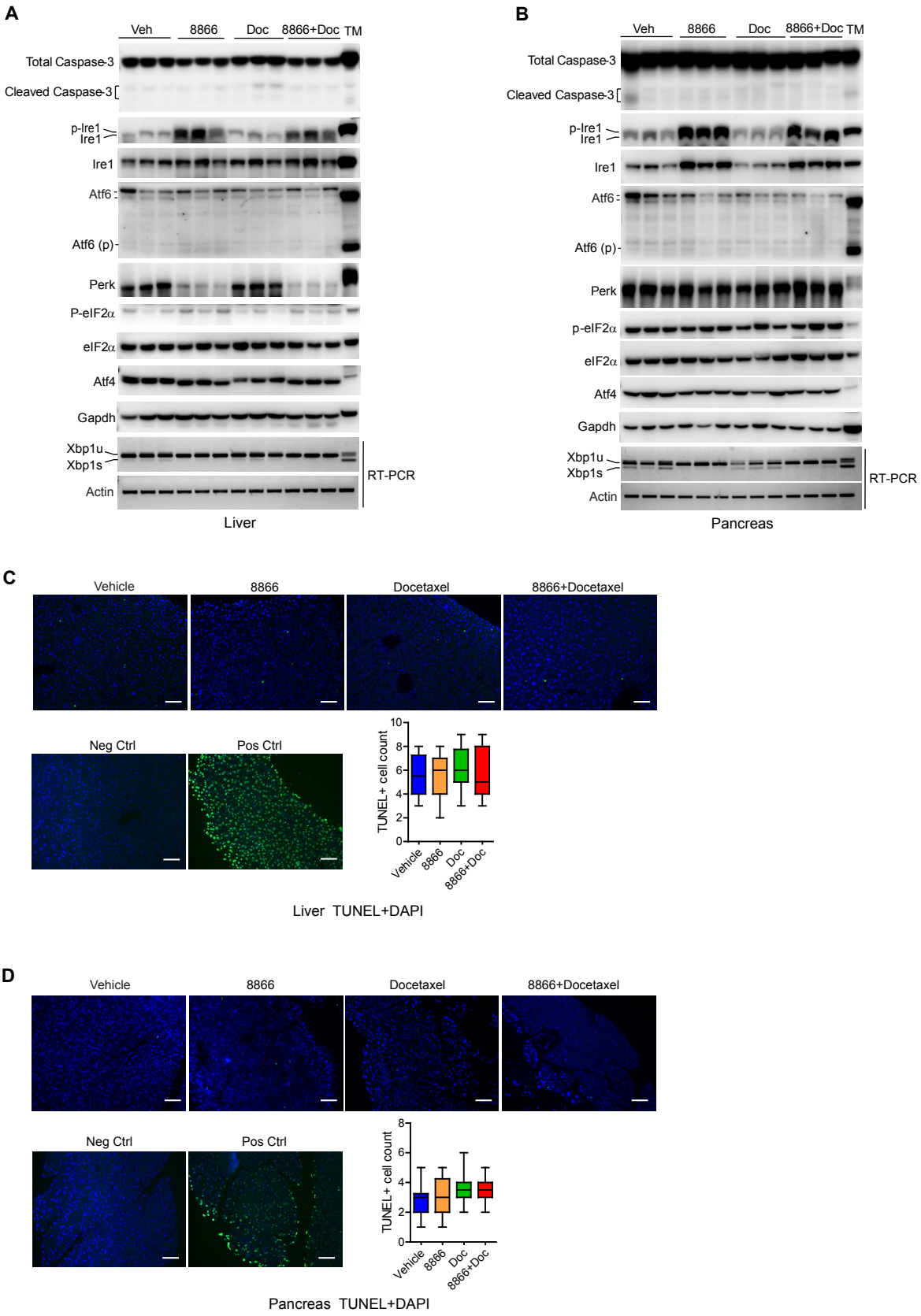

Supplemental Figure 13. The effect of 8866 +/- docetaxel treatments on the liver and pancreas of MC1 PDX tumor-bearing mice. (**A**, **B**) Immunoblot and *Xbp1* splicing assays of liver (**A**) and pancreas (**B**) tissues from MC1 PDX tumor-bearing SCID/Beige mice treated with vehicle, 300 mg/kg 8866 (daily oral gavage), docetaxel (10 mg/kg, weekly i.p. injection), or the combination of 8866 and docetaxel. Mice undergoing monotherapy also received vehicle. Phos-tag SDS-PAGE gels was used to detect Ire1 phosphorylation. Gapdh was used as loading control for immunoblot and *Actin* was used as loading control for RT-PCR. *n*=3 in each group. NIH3T3 cells treated with 5 μg/ml tunicamycin (TM) for 6 h were used as control. (**C**, **D**) TUNEL staining of liver (**C**) and pancreas (**D**) tissues from MC1 PDX tumor-bearing SCID/Beige mice treated as in (**A**, **B**). Tissue sections incubated with TUNEL reaction buffer without dTd enzyme served as negative control. Tissue sections treated with DNase I served as positive control. Scale bar, 100 μm. TUNEL positive cells were quantitated from more than 15 random views. No statistically significant differences were observed among the groups using one-way ANOVA with Turkey's multiple comparison test.

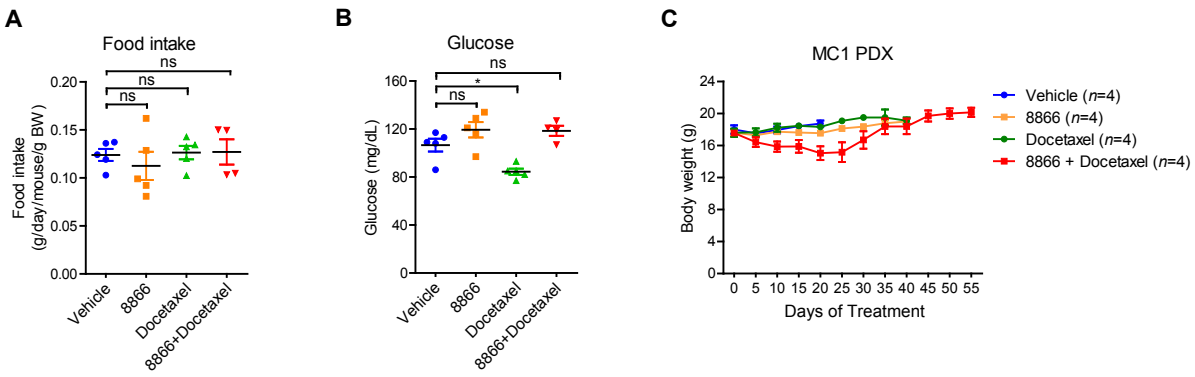

Supplemental Figure 14. The effects of 8866 +/- docetaxel treatments on MC1 PDX tumor-bearing mice. (**A**, **B**) Food intake (**A**) and blood glucose levels (after overnight fasting) (**B**) of MC1 PDX tumor-bearing SCID/Beige mice treated with vehicle, 300 mg/kg 8866 (daily oral gavage), docetaxel (10 mg/kg, weekly i.p. injection), or the combination of 8866 and docetaxel for 20 days. Mice undergoing monotherapy also received vehicle. (**C**) Body weight of mice treated as in **Figure 7B**. All data are presented as mean ± s.e.m of biological replicates. p value was calculated using one-way ANOVA with Turkey's multiple comparison test (**A**, **B**). ns, not significant; * $p<0.05$.

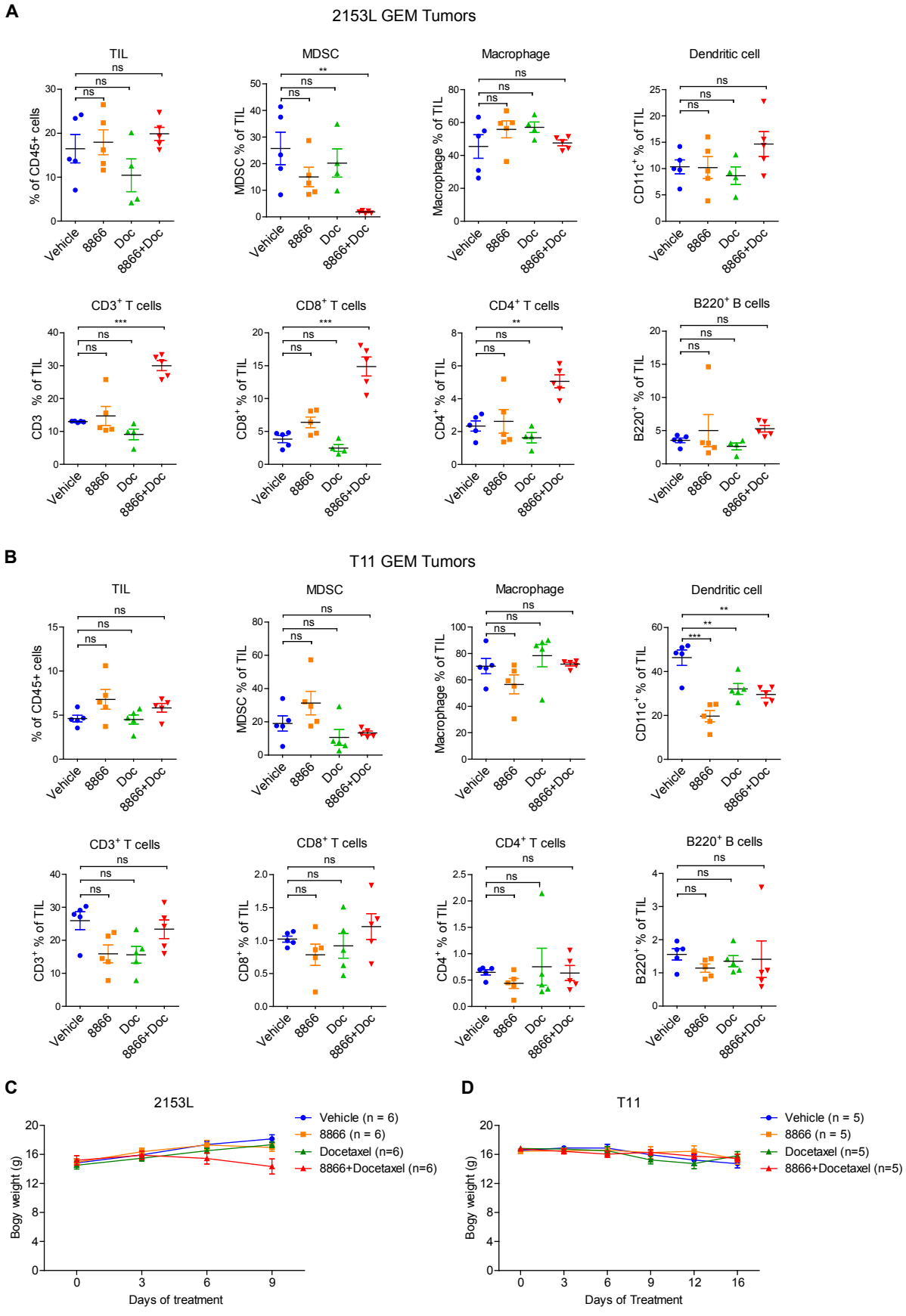

Supplemental Figure 15. The effects of 8866 +/- docetaxel treatments on the immune surveillance in the syngeneic GEM tumors. (**A**, **B**) Immunophenotyping of *p53*-null GEM tumors 2153L (**A**) and T11 (**B**) that were transplanted into BALB/c mice and treated with vehicle, 300 mg/kg 8866 (daily oral gavage), docetaxel (10 mg/kg, weekly i.p. injection), or the combination of 8866 and docetaxel. Mice undergoing monotherapy also received vehicle. Tumor-infiltrating leukocytes (TIL) were defined as CD45+ cells. Percentages of MDSCs (myeloid-derived suppressor cells, CD11b+ Gr-1+), macrophage (CD11b+ Gr-1- F4/80+), CD11c+ dendritic cells, CD3+ T cells, CD8+ T cells, CD4+ T cells, or B220+ B cells in CD45+ TILs are shown. Data are presented as mean ± s.e.m. of biological replicates. p value was calculated using one-way ANOVA with Turkey's multiple comparison test. ns, not significant; ** p<0.01; *** p<0.001. (**C**, **D**) Body weight of BALB/c mice bearing 2153L (**C**) or T11 (**D**) GEM tumors treated as in (**A**, **B**). All data are presented as mean ± s.e.m of biological replicates.

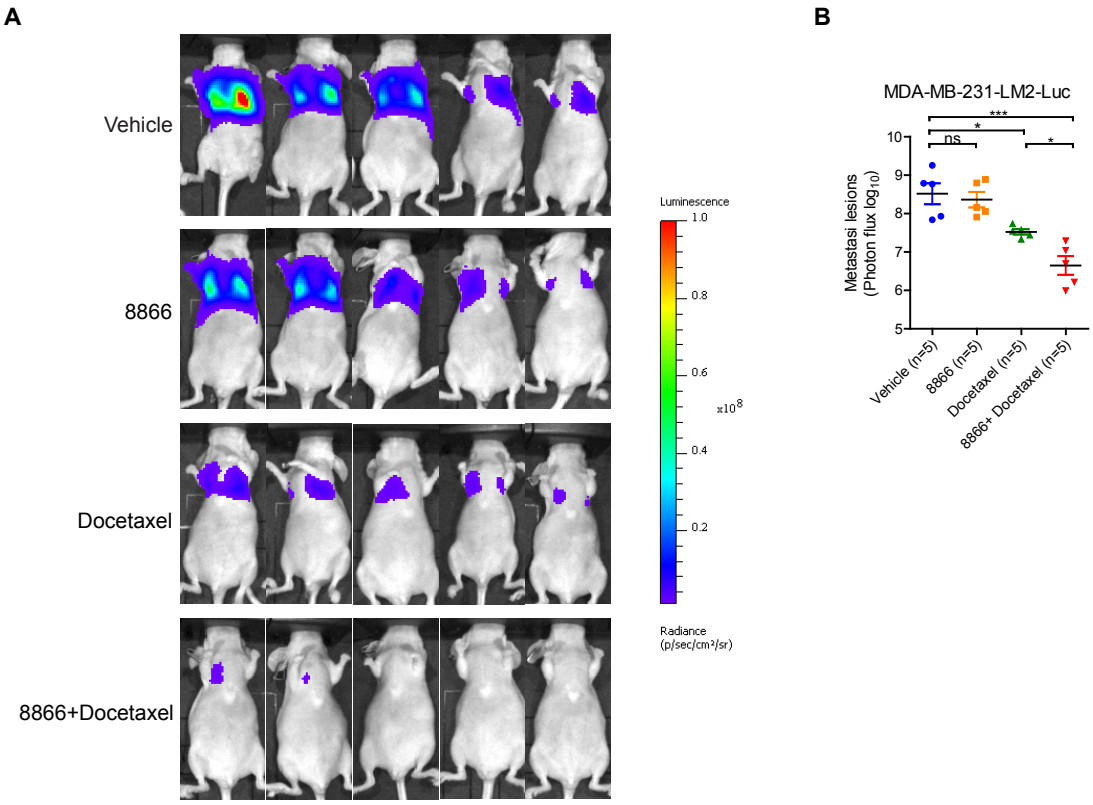

Supplemental Figure 16. The effects of 8866 treatments on lung metastasis.
MDA-MB-231-LM2-Luc cells were injected into the athymic nude mice through tail vein. Mice were then treated with vehicle, 300 mg/kg 8866 (daily oral gavage), docetaxel (10 mg/kg, weekly i.p. injection), or the combination of 8866 and docetaxel for 5 weeks. Mice undergoing monotherapy also received vehicle. *n*=5 in each group. (**A**) Representative bioluminescent images of lung metastasis formed by MDA-MB-231-LM2-Luc cells. Bioluminescent images were obtained 5 weeks after treatment. (**B**) Quantification of imaging studies as in **A**. Data are presented as mean ± s.e.m. p value was calculated using one-way ANOVA with Turkey's multiple comparison test. ns, not significant; * $p<0.05$; *** $p<0.001$.

Supplemental Table 1. Sequences of DNA Oligonucleotides

Name	Sense Strand / Sense Primer (5'-3')	Antisense Strand / Antisense Primer (5'-3')
Primers for shRNA construct generation		
sh*LacZ*	CCGGCGCTAAATACTGGCAGGCGTTCTGCAGA ACGCCTGCCAGTATTTAGCGTTTTT	AATTAAAAACGCTAAATACTGGCAGGCGTTC TGCAGAACGCCTGCCAGTATTTAGCG
sh*XBP1*	CCGGGACCCAGTCATGTTCTTCAAACTCGAGT TTGAAGAACATGACTGGGTCTTTTTG	AATTCAAAAAGACCCAGTCATGTTCTTCAAAC TCGAGTTTGAAGAACATGACTGGGTC
sh*IRE1*	CCGGGCAGGACATCTGGTATGTTATCTCGAGA TAACATACCAGATGTCCTGCTTTTTG	AATTCAAAAAGCAGGACATCTGGTATGTTATC TCGAGATAACATACCAGATGTCCTGC
sh*PERK*	CCGGTAGCAGCAATCCCTAATATATCTCGAGA TATATTAGGGATTGCTGCTATTTTTG	AATTCAAAAATAGCAGCAATCCCTAATATATC TCGAGATATATTAGGGATTGCTGCTA
sh*ATF6*-1	CCGGGCAGCAACCAATTATCAGTTTCTCGAGA AACTGATAATTGGTTGCTGCTTTTTG	AATTCAAAAAGCAGCAACCAATTATCAGTTTC TCGAGAAACTGATAATTGGTTGCTGC
sh*ATF6*-2	CCGGCAGACAGTACCAACGCTTATGCTCGAGC ATAAGCGTTGGTACTGTCTGTTTTTG	AATTCAAAAACAGACAGTACCAACGCTTATG CTCGAGCATAAGCGTTGGTACTGTCTG
Primers for luciferase reporter generation		
IRE1- promoter	ATATAACGCGTCCTAGGATAAGTTAGATAC	TATATCCATGGCGAGGACTCGGCCCTGG
IRE1- enhancer	ATATAACGCGTGGTCTGCATGTCTTGTTTCT	TATATAGATCTTTCTGCAAGAGCAGGCATTA
Primers for RT-qPCR		
IRE1	AGTATGTGGAGCAGAAGGAC	GTTGTGTGGCTTTAGGTCTC
XBP1s	CTGAGTCCGCAGCAGGTG	TCCAAGTTGTCCAGAATGCC
XBP1 total	GGCATCCTGGCTTGCCTCCA	GCCCCCTCAGCAGGTGTTCC
ACTIN	GCGAGAAGATGACCCAGATC	CCAGTGGTACGGCCAGAGG
DNAJB9	TCGGCATCAGAGCGCCAAATCA	ACCACTAGTAAAAGCACTGTGTCCAAG
SEC63	CCTCCACTTACCTGCCCATA	GGTTCCGGGCCATTACTATT
HSPA5	GACGGGCAAAGATGTCAGGA	GCCCGTTTGGCCTTTTCTAC
DNAJC3	CTCAGTTTCATGCTGCCGTA	TTGCTGCAGTGAAGTCCATC
MYC	GCCACGTCTCCACACATCAG	TCTTGGCAGCAGGATAGTCCTT
SEC61A1	TGGAAGTCATCAAGCCCTTC	AGAGGGTGATAGCGGTCCAC
NCL	GCGAAGGCAGGTAAAAATCA	GACGACCTCTTCTCCACTGC
CDK4	TACTGAGGCGACTGGAGGCT	AGTTCGGGATGTGGCACAG
ODC1	CAAAGGCAACTCTCCAGGAA	GGCTGCGACTCAGGCTC
HSPD1	GTTGAAGGATCTTTGATAGTTG	TTCTCTTCTTTAGGAATTTCTG
DDX18	TTCATGGGCTTTTGTTTTGA	GATCGAGAAGCGGAACCTC
DNAJC10	GGCCAGTATGAAAGCTGGAA	GTGAACAGCCTGGGGAGTAA
PDIA3	AAGCTCAGCAAAGACCCAAA	CACTTAATTCACGGCCACCT
ERN2	CGTGCTGTGAGGAACAAGAA	GGGAAGCGGTTTGTGAAGTA
CHOP	CTGCTTCTCTGGCTTGGCTG	GCTCTGGGAGGTGCTTGTGA
GADD34	CCCAGAAACCCCTACTCATGATC	GCCCAGACAGCCAGGAAAT
EDEM1	TTGACAAAGATTCCACCGTCC	TGTGAGCAGAAAGGAGGCTTC
PDIA2	GATCAGCGGCCAGTTAAGAC	GATGTCCTCGTGGTCTTGGT
SEL1L	AGTTGGACAGAGTGGGCTTG	ATCCACCCAGCCTTGTTCAG
SYVN1	TACGCCGTCACAGAGACTTG	TGCGTTCCATAAAGTCCACA
CD59	GGAATCCAAGGAGGGTCTGT	TGCAGTCAGCAGTTGGGTTA
DGAT2	CATACGGCCTTACCTGGCTA	ATTGCCACTCCCATTCTTTG
PMP22	CCTGTCGATCATCTTCAGCA	AGCACTCATCACGCACAGAC
CDKN1A	GCCATTAGCGCATCACAGT	TGCGTTCACAGGTGTTTCTG
CDKN2B	ATGCGCGAGGAGAACAAG	CTCCCGAAACGGTTGACTC
Sec61a1 (mouse)	CTGGCGGTAGAATGCCTCT	TGAGACCATTGTGTGGAAGG
Ddit3 (mouse)	GTCCCTAGCTTGGCTGACAGA	TGGAGAGCGAGGGCTTTG
Dnajb9 (mouse)	CCCCAGTGTCAAACTGTACCAG	AGCGTTTCCAATTTTCCATAAATT
Hspa5 (mouse)	TCATCGGACGCACTTGGA	CAACCACCTTGAATGGCAAGA
Gadd34 (mouse)	AGGACCCCGAGATTCCTCTA	CTTCGATCTCGTGCAAACTG
Actin (mouse)	TACCACCATGTACCCAGGCA	CTCAGGAGGAGCAATGATCTTGAT

Primers for XBP1 splicing assay

XBP1 splicing	CCTGGTTGCTGAAGAGGAGG	CCATGGGGAGATGTTCTGGAG
ACTIN	GCGAGAAGATGACCCAGATC	CCAGTGGTACGGCCAGAGG
Xbp1 splicing (mouse)	ACACGCTTGGGAATGGACAC	CCATGGGAAGATGTTCTGGG
Actin (mouse)	TACCACCATGTACCCAGGCA	CTCAGGAGGAGCAATGATCTTGAT

Primers for ChIP-qPCR

DNAJB9	CTCGTCTGTCGACTCACTTC	TGGAAAACTGTTGTTGCTGC
P4HB	TTGGGGTGACGCAATTTCC	CATGCCTCGGTGAGTGTCT
DNAJC10	TCAACCTAAACCTACACCGC	GGTACCGGTAGGTTCCTCA
DNAJC3	ATCAAATAGTCCCACTCGCC	GATAACGTGGAAGCACGAGA
EDEM1	TTCCTTAAAGGGGAAGCGAG	AAGACGAGCCACAATACTCC
SERP1	TTGCCTTTGAGAACTACCCG	CCGATTGCCACGCTATATCA
HERUPD1	CCAAACATGGCCACCGAA	CAGAACGCTCTGTGGCTG
HSPA5	CGAAACACCCCAATAGGTCA	ATATAAGCCGAGTAGGCGAC
PDIA3	TAGAACTCACGGACGACAAC	AAGAACTCGACGAGCATGAG
SEC61A1	CTGTTACGTGTATGGGAGCC	CAGACTTGGTAACGCGAGAG
ERN2	CTTATGGAGAACTTGCCACG	CTGGTGCAATGATAAAGAGCG
MBTPS1	GGGGCTGTTTACTCCCAAC	AAATGTCGCGAGACCTTCGT
VEGFA (Ctrl)	TGAGGGTTCATCAAGCTGGTGTCT	TTGGAGAGGGCAGTGCTTAACTCA
SEL1L	ATGTCCGTGAGTCGTGGTC	GCTTCTGGTCCAATCACCAT
SYVN1	CCGTAGACATCACCCCAGAT	GGGTCAGACACCTCACTTCC
TSEN34	CCAAAGAGGATGAGACCAGTG	TGGTGGGGAGTACAGAGAAGA
ATP50	TACTGCCGCAGAGTTTGATCT	CCCTTCCTGGCATCTTAGGTA
NDUFA3	TCAAGAATGCCTGGGACAAG	ATGGGGATAGATAAGGGGATG
IRE1-P1	TAACTGTCCAGGCTTCTTGG	GTGACCCTGTAACATCAGCA
IRE1-P2	TTTCCCAGCCACAGACAAG	GGCTGTAAAGGACCAGGC
IRE1-P3	CCTCATGAGCGAAGCCAG	CTATAAGCGCTGGGTGCC
IRE1-P4	GAGACGAATGATAGGGCCTG	ACGCTCACATCCTGAACAAT
IRE1-E1	GAGGCTTATTCCAGGTGCTT	GATTCAGGACATTGGCAGGA
IRE1-E2	TGAGTTGTTTGTTTGCTGCC	CCCAGCTCCTATACAAAGGC
IRE1-E3	TCTGTCACCATAAGCAGAGC	AGCGATGAGGTATTTCCAGC
IRE1-E4	ATGTAGAGCTACTCCAGGCA	GGATGGATGCAGAACGAAGA